Convective structures in a two-layer gel-liquid excitable medium

Vicente Pérez-Villar,* Alberto P. Muñuzuri, and Vicente Pérez-Muñuzuri
Group of Nonlinear Physics, Faculty of Physics, University of Santiago de Compostela, 15706 Santiago de Compostela, Spain
(Received 27 July 1999)

The onset of convection due to wave propagation is investigated in the framework of the Belousov-Zhabotinsky reaction. Numerical calculations are based on a three variable Oregonator model coupled with the Navier-Stokes hydrodynamic equations under the Boussineq approximation for a system consisting of two layers, a liquid and a gel, both in close contact through an interface where chemical concentration exchange is allowed. The influence on the formation of convective rolls associated to wave front propagation is studied in terms of the exchange rate through the interface, the liquid layer width, and the coupling strength between the fluid flow and chemical dynamics. Waves are initiated on the surface of the gel and this perturbation is allowed to propagate into the liquid initiating either two counterrotating convective cells (at both sides of the front) or a disordered pattern.

PACS number(s): 47.20.Bp, 47.70.Fw, 82.20.Mj

I. INTRODUCTION

Chemical oscillations and pattern formation have been interesting and fruitful areas of research for the past two decades [1,2]. Many phenomena, such as target patterns, spiral waves, or periodic plane wave trains can be described in terms of reaction-diffusion mechanisms. Nevertheless, some work has been done to include the hydrodynamic effects that develop when experiments are performed in aqueous solutions. Convection may play a role in these processes since different chemical compositions induce density gradients produced by thermal and chemical gradients in the vicinity of the reaction front. In fluid problems such as the Rayleigh-Bénard problem of a fluid heated from below, such buoyancy driven convection can take the form of traveling waves or oscillatory instabilities among other different pattern formation [3]. Involving both hydrodynamic and reaction-diffusion effects, convection in autocatalytic systems is a potentially rich and fruitful area of investigation.

Experiments in the iodate-arsenous acid system [4] have shown that fronts traveling in vertical capillary tubes show that steady nonsymmetric convection can exist in the moving-front frame. This convection is driven by the buoyancy of the lighter reacted fluid below the ascending front, while the effect is different for descending fronts. In addition, Epstein and co-workers [5] have shown that the front velocity depends on the direction of propagation with respect to the gravitational force. Numerical studies with an Oregonator reaction-diffusion model coupled with the Navier-Stokes hydrodynamic equations have been performed by Vasquez and co-workers [6] to reproduce the formation of convective structures associated to the reaction fronts. In this sense, Biktashev *et al.* [7] numerically showed that the presence of a constant advective flow in the direction of movement of a wave front can increase or decrease its wave velocity. Analogously, the action of an electric field on a chemical excitable medium, where the role of the advection velocity is played by the electric field, is formally equivalent to that for reaction diffusion with convective flow [8]. A series of delicate experiments by Miike and co-workers [9] observed oscillatory hydrodynamic flow and periodic deformation of wave fronts induced by spiral wave propagation. Also, they showed the formation of convective rolls associated with chemical waves in the framework of the Belousov-Zhabotinsky (BZ) reaction even in the absence of external factors such as surface tension, surface evaporative cooling, or even inhomogeneities in the reagents that may affect the onset of convection. These convective structures may interact with the spatial patterns finally leading to the development of autowave chaos (chemical turbulence) in a nonhomogeneous medium [10,11].

In the last decade, the introduction of gelled media with inmobilized catalyst (ferroin, ruthenium, etc.) covered by a catalyst-free solution, partially solved the formation of convective cells since reaction and then front propagation occurs at the interface between the liquid and the gel. Nevertheless, recent experiments by Markus *et al.* [12] and Ouyang and Fleselles [13] reported the formation of disordered waves in the light-sensitive BZ reaction in which hydrodynamic flow and/or inhomogeneities played an important role. Therefore, the purpose of this paper is to analyze the onset of convection due to wave propagation in a system consisting of two media; a liquid and a gel. Since the catalyst is inmobilized into the gel, we only consider flow motion into the liquid part of the medium. A wave front propagating through the common interface between the liquid and the gel leads to the formation of steady convective cells that can exist in the frame of the moving front and may be unstabilized depending on the relative values of the exchange rates of chemicals through the interface and the ion diffusivities, as well as on other factors as the liquid layer depth and the coupling strength between the fluid flow dynamics and the chemical reaction kinetics.

II. MODEL

A. Equations of motion

In order to simulate the behavior of a gel-liquid system, we considered two independent media in the system (the

*Electronic address: fmvpv@usc.es

 © 2000 The American Physical Society

upper part liquid and the lower gel). In both of them, the Belousov-Zhabotinsky (BZ) reaction takes place, but fluid motion only develops in the liquid medium (placed above the gel part). The only exchange of reactants is through the common boundary. Even if a complete description of the system requires the use of a three-dimensional geometry, we will confine our attention to the simpler two-dimensional geometry, with the z axis in the direction of gravity. In the lower part of the system (gel), only diffusion of the reactants is considered, meanwhile in the upper part (liquid) we also included the convective motions due to the concentration gradients of the chemicals.

In order to describe the reaction-diffusion process due to the BZ reaction, a three-variable Oregonator model has been used [14,15] whose source, terms F,G, and H are given by

$$F(\mathbf{x})=\frac{1}{\epsilon}[w(q-u)+u-u^2],$$

$$G(\mathbf{x})=u-v, \tag{1}$$

$$H(\mathbf{x})=\frac{1}{\epsilon'}[-w(q+u)+fv],$$

where $\mathbf{x}$ is the state vector of variables (u,v,w). u,v, and w represent the dimensionless concentrations of $[HBrO_2]$, [ferroin], and $[Br^-]$ respectively, and f,q,ϵ,ϵ' are constants related to the chemical kinetics [15–17]. For a typical recipe, we have used a scaling with a spatial unit (s.u.) of 0.018 cm and a time unit (t.u.) of 21 s [6,17] using the ''Lo'' kinetic values given by Keener and Tyson [17]. Under this scaling, those constants are $f=3$, $q=0.002$, $\epsilon=0.01$, and $\epsilon'=0.001$. For this particular choice of parameters the Oregonator model exhibits the dynamics of an excitable medium [14,15].

The nonconvective part of the medium (gel) is located at the lower part of the system. Here, the z coordinate moves from z_{1g} (corresponding to the lower layer of gel) to z_{2g} (the upper layer of gel in the system). The equations describing the dynamics in the nonconvective part of the medium (gel) are given by

$$\frac{\partial u_g}{\partial t}=F(\mathbf{x}_g)+D_{ug}\nabla^2 u_g,$$

$$\frac{\partial v_g}{\partial t}=G(\mathbf{x}_g)+D_{vg}\nabla^2 v_g, \tag{2}$$

$$\frac{\partial w_g}{\partial t}=H(\mathbf{x}_g)+D_{wg}\nabla^2 w_g,$$

where D_{ug},D_{vg}, and D_{wg} are the diffusion coefficients for the u,v, and w species in the gel.

Placed right above the gel lies the convective part of our system (liquid); $z_{1l}\leqslant z\leqslant z_{2l}$. $z=z_{1l}$ corresponds to the lower layer of the liquid system in close contact with the gel and $z=z_{2l}$ is the upper layer in the liquid system. Since we assume that fluid motion can take place in the liquid medium due to reaction and diffusion processes that develop in there, the Navier-Stokes equations under the Boussinesq approximation and the BZ reaction-diffusion equations have been coupled leading to the following set of equations:

$$\left(\frac{\partial}{\partial t}+\mathbf{V}\cdot\boldsymbol{\nabla}\right)u_l=F(\mathbf{x}_l)+D_{ul}\nabla^2 u_l,$$

$$\left(\frac{\partial}{\partial t}+\mathbf{V}\cdot\boldsymbol{\nabla}\right)v_l=G(\mathbf{x}_l)+D_{vl}\nabla^2 v_l,$$

$$\left(\frac{\partial}{\partial t}+\mathbf{V}\cdot\boldsymbol{\nabla}\right)w_l=H(\mathbf{x}_l)+D_{wl}\nabla^2 w_l, \tag{3}$$

$$\left(\frac{\partial}{\partial t}+\mathbf{V}\cdot\boldsymbol{\nabla}\right)\mathbf{V}=-\mathbf{g}\frac{\rho-\rho_0}{\rho_0}-\frac{1}{\rho_0}\boldsymbol{\nabla}P_r+\nu\nabla^2\mathbf{V},$$

$$\boldsymbol{\nabla}\cdot\mathbf{V}=0,$$

where D_{ul},D_{vl}, and D_{wl} are the diffusion coefficients of the u,v, and w variables in the liquid part. $\mathbf{V}=(V_x,V_z)$ is the fluid velocity, P_r is the reduced pressure related to the conventional pressure p by $P_r=p-\rho_0(g_x x+g_z z)$, and $\mathbf{g}=(g_x,g_z)$ is the acceleration of gravity with $g_x=0$, $g_z=g$ for our choice of axes. ν is the kinematical viscosity, and ρ and ρ_0 are the densities of the liquid system and of the bulk fluid, respectively. By writing equations in this form, all hydrodynamic variables are expressed in terms of the scaling of Eq. (1). That is, $g=980\ \text{cm s}^{-2}\times(21\ \text{s})^2/(0.018\ \text{cm})=2.4\times10^7$, and $\nu=9.2\times10^{-3}\ \text{cm}^2\ \text{s}^{-1}\times(21\ \text{s})/(0.018\ \text{cm})^2=5.96\times10^2$.

In order to close the proposed model for the liquid, Eq. (3), a relationship between the density and the variables u,v, and w must be established. Density changes as a consequence of the chemical reaction that takes place into the liquid layer. Although the chemical reactions here involved produce heat fluxes in the medium, their effect was not considered in this paper, assuming the temperature to remain constant during the proccess. Since the total mass of the solution remains constant, the density change must be a result of a volume change due to the reaction. Thus, it is possible to write

$$V=V_0+(u-u_0)\delta V_u+(v-v_0)\delta V_v+(w-w_0)\delta V_w, \tag{4}$$

where V is the volume of the solution with concentrations (u,v,w), V_0 is the initial volume of the reaction with concentrations (u_0,v_0,w_0) equal to the steady state values of the variables. For our choice of parameters and in dimensionless form we have $u_0=v_0=3.998\times10^{-4}$, $w_0=1.998$. $\delta V_u,\delta V_v$, and δV_w represent the molar volume change due to the reaction. In general, the density variation due to the change in chemical composition is quite small for the most known reactions. We may, therefore, assume a linear dependence of the density on the chemical concentrations

$$\rho=\rho_0[1-\sigma_u(u-u_0)-\sigma_v(v-v_0)-\sigma_w(w-w_0)], \tag{5}$$

where $\sigma_u=\delta V_u/V_0$, $\sigma_v=\delta V_v/V_0$, and $\sigma_w=\delta V_w/V_0$ are the coefficients of linear expansion due to the compositional change of $[HBrO_2]$,[ferroin], and $[Br^-]$, respectively. The three-variable Oregonator model is a very simplified model

for the BZ reaction, it may not precisely account for the chemical dependence of the hydrodynamic fluid, furthermore, there are no experimental results about the relative importance of the σ_u, σ_v, and σ_w. In this paper, we assume that the density only depends on the concentration of the $[HBrO_2]$ and $[Br^-]$ and set $\sigma_u = \sigma_w = \sigma(\sigma_v = 0)$ [18]. Then, Eq. (5) simplifies to

$$\rho = \rho_0[1 - \sigma(u - u_0) - \sigma(w - w_0)]. \tag{6}$$

Positive or negative values of σ are related to a greater or smaller density in the liquid solution where the reaction takes place [19]. σ can be obtained from experimental measurements and its value dramatically changes depending on the reaction or catalysts used. In our case, we set $\sigma = 2.0 \times 10^{-5}$ for a typical BZ reaction with ferroin as a catalyst [4].

Now, as usual in fluid physics, the reduced pressure P_r can be eliminated from Eqs. (3) by introducing the stream function ψ defined as

$$V_x = \frac{\partial \psi}{\partial z}, \quad V_z = -\frac{\partial \psi}{\partial x} \tag{7}$$

and the vorticity $\omega = -\nabla^2 \psi$, then, the equations describing the dynamics in the liquid (3) can be rewriten as

$$\begin{aligned} \frac{\partial u_l}{\partial t} &= F(\mathbf{x_1}) + J(\psi, u_l) + D_{ul}\nabla^2 u_l, \\ \frac{\partial v_l}{\partial t} & G(\mathbf{x_1}) + J(\psi, v_l) + D_{vl}\nabla^2 v_l, \\ \frac{\partial w_l}{\partial t} &= H(\mathbf{x_1}) + J(\psi, w_l) + D_{wl}\nabla^2 w_l, \\ \frac{\partial \omega}{\partial t} &= J(\psi, \omega) + \sigma g\left(\frac{\partial u_l}{\partial x} + \frac{\partial w_l}{\partial x}\right) + \nu \nabla^2 \omega, \\ \omega &= -\nabla^2 \psi, \end{aligned} \tag{8}$$

where the Jacobi operator

$$J(f_1, f_2) = \frac{\partial f_1}{\partial x}\frac{\partial f_2}{\partial z} - \frac{\partial f_2}{\partial x}\frac{\partial f_1}{\partial z} \tag{9}$$

has been used.

Finally, the exchange of chemicals between the gel and the liquid part of the system is considered to be only through the upper layer of the gel system $z = z_{2g}$ and the lower layer of the liquid system $z = z_{1l}$. To consider this exchange of matter, we included an additional flux term proportional to the exceeding value of the variable in the gel comparing with the value of the same variable in the liquid [20]. Thus, for $z = z_{2g}$, the equations describing the dynamics of this layer are

$$\begin{aligned} \frac{\partial u_g}{\partial t} &= F(\mathbf{x}_g) + D_{ug}\nabla^2 u_g - \beta_u(u_g - u_l^*), \\ \frac{\partial v_g}{\partial t} &= G(\mathbf{x}_g) + D_{vg}\nabla^2 v_g - \beta_v(v_g - v_l^*), \\ \frac{\partial w_g}{\partial t} &= H(\mathbf{x}_g) + D_{wg}\nabla^2 w_g - \beta_w(w_g - w_l^*), \end{aligned} \tag{10}$$

where $u_l^* = u_l(z_{1l})$, $v_l^* = v_l(z_{1l})$, and $w_l^* = w_l(z_{1l})$.

As well for the lower layer in the liquid medium $z = z_{1l}$,

$$\begin{aligned} \frac{\partial u_l}{\partial t} &= F(\mathbf{x_1}) + J(\psi, u_l) + D_{ul}\nabla^2 u_l - \beta_u(u_l - u_g^*), \\ \frac{\partial v_l}{\partial t} &= G(\mathbf{x_1}) + J(\psi, v_l) + D_{vl}\nabla^2 v_l - \beta_v(v_l - v_g^*), \\ \frac{\partial w_l}{\partial t} &= H(\mathbf{x_1}) + J(\psi, w_l) + D_{wl}\nabla^2 w_l - \beta_w(w_l - w_g^*), \\ \frac{\partial \omega}{\partial t} &= J(\psi, \omega) + \sigma g\left(\frac{\partial u_l}{\partial x} + \frac{\partial w_l}{\partial x}\right) + \nu \nabla^2 \omega, \\ \omega &= -\nabla^2 \psi, \end{aligned} \tag{11}$$

where $u_g^* = u_g(z_{2g})$, $v_g^* = v_g(z_{2g})$, and $w_g^* = w_g(z_{2g})$.

β_u, β_v, and β_w are the matter transfer coefficients or exchange coefficients, for $[HBrO_2]$, [ferroin], and $[Br^-]$, respectively, between the gel and the liquid and they are responsible for the exchange of matter among the two media. They are similar to the reciprocal residence time used in coupled CSTR systems. We set the dimensionless diffusion coefficients $D_{ug} = D_{wg} = 1$ and since matter exchange is allowed to occur at the interface between both media and in general $\beta_v \neq 0$, we admit that ferroin v can diffuse into the gel but at lower values than u and w; $D_{vg} = 0.03$. On the other hand for the liquid medium, since density is lower than for the gel system, we consider greater diffusivities; $D_{ul} = D_{wl} = 1.4$ and $D_{vl} = 0.4$. The same reasoning can be applied to the exchange coefficients between gel and liquid and consequently we will consider from now on $\beta_u = \beta_w$. We will show later in Sec. III that the main influence on wave propagation, both in the gel and the liquid media, is due to the values of the exchange coefficients and not on the specific values of the dimensionless diffusion coefficients. Nevertheless, we will always consider that ferroin diffuses slower than the other two components in the reaction. Equations (1), (2), (8), (10), and (11) completely define our problem.

B. Initial and boundary conditions

The boundary conditions at the top and bottom of each medium are no-slip boundary conditions for the fluid velocity (i.e., zero-flux boundary conditions for the stream function and vorticity) and zero-flux boundary conditions for the chemical concentrations. We also require periodic boundary conditions for all variables involved in our equations at the left and right boundaries of the domain.

The set of equations (2), (10) have been integrated using an alternating direct implicit (ADI) method, while Eqs. (8)

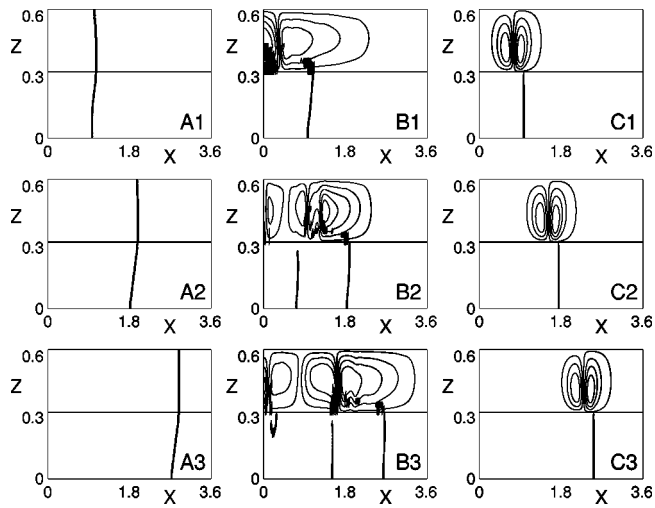

FIG. 1. Wave propagation through a gel-liquid system. (A) $\sigma = 0.0$ (no convection), (B) $\sigma = 2.0\times10^{-5}$, and $\beta_u = \beta_w = 0.6$ (turbulent regime), (C) $\sigma = 2.0\times10^{-5}$ and $\beta_u = \beta_w = 0.5$ (steady propagation of the wavefront together with two counterrotating vortices in the liquid layer). Times for figures are (1) 0 s, (2) 105 s, and (3) 210 s. (Other parameters: $\beta_v = 0.25$. Units in both axis are in cm.) The upper part of the medium in each subplot (above the solid stright line) corresponds to the liquid medium while the bottom (below the line) is the gel. In all subplots the pattern formed by the values of the u variable is plotted (white means 0 while black is 0.8, gray colors are linearly interpolated from these). We also plot the stream function in the liquid part (contour lines are plotted every 9.3 mm^2/min, negative values are in front of the propagating wave front while positive values are at the back). In all cases, the wave front propagates towards increasing values of X. Waves propagating towards negative values of X were systematically eliminated in order to be able to follow the propagation of the main wave for longer periods of time.

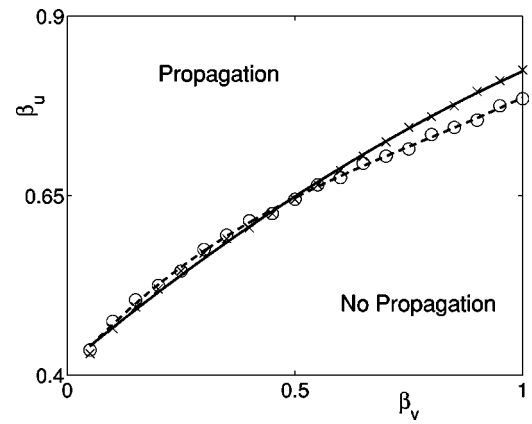

FIG. 2. Critical values of the transfer matter coefficients. β_u, versus β_v for wave propagation inside the liquid medium. Two cases are plotted; no convection [$\sigma = 0.0$, marked with $\times$] and convection ($\sigma = 2.0\times10^{-5}$, marked with $\bigcirc$). (Solid and dashed lines are just a guide for the eye).

and (11) were integrated with a simultaneous over-relaxation (SOR) method coupled to the ADI method [21]. The spatial step sizes are $\Delta x = \Delta z = 1$ s.u. while the time step is $\Delta t = 10^{-5}$ t.u. The mesh sizes for the gel slab were $L_x \times L_z^g = 200\times16$. Since the size L_z^l for the liquid layer affects the wave propagation, a range of values were selected; $2 \leqslant L_z^l \leqslant 16$ for research purposes. The value of L_x was chosen so that higher mesh sizes do not affect the obtained results.

Initially, chemical concentrations are supposed to be in the steady state with no fluid flow anywhere (so, the vorticity and the stream function were set equal to zero for all the mesh points). A front is generated only within the gel slab by increasing the values of the concentration variables to $u_g = 0.5$, $v_g = 0.05$, and $w_g = 1.0$ at $L_x/4$. Two pulses are then generated into the gel medium which propagate in opposite directions although the left one is annihilated. The exchange matter with the liquid layer is allowed to occur when the front reaches the position $L_x/2$.

III. RESULTS

The main influence of fluid dynamics on chemical wave propagation is shown in Fig. 1 for a two-layer gel-liquid excitable medium. The temporal evolution (from top to bottom in Fig. 1) of a wave front is shown for three situations; (A) $\sigma = 0$, the density does not depend on the chemical species and the fluid flow dynamic is uncoupled from the reaction kinetics under the Boussinesq approximation used in this paper, (B) and (C) $\sigma \neq 0$ for two different transfer matter coefficients β_u. For $\sigma = 0$, the front in the gel excites the liquid region at its bottom and this excitation finally develops into a wave front, whose shape (as well as the wave front into the gel medium) remains unchanged. For the selected set of parameters, the wave velocity in the liquid layer is nearly twice the velocity in the gel, so the front in the gel medium is folded as its velocity near the interface should match the wave velocity value for the liquid medium [see Figs. 1(A2), 1(A3)]. This particular case reproduces experiments by Zhabotinsky and co-workers [22] where they describe wave propagation in a medium composed by two parts with different diffusion coefficients and without convection.

When $\sigma \neq 0$, a complex fluid dynamic behavior develops, Figs. 1(B1)–1(B3). First, a chemical wave front is induced in the liquid medium at the top boundary of the gel layer as a consequence of the mass transfer at the interface. Then, density gradients due to chemical gradients in the vicinity of the reaction front originate and give rise to two counter-rotating convective type vortices. These convective fluid vortices trap chemicals from the bottom side of the liquid layer which are reinjected into the back and front of the initial wave front, at the gel surface where new wave fronts are initiated, then repeating the process depicted above. The new wave initiated in front of the original wave front dies out as the old one reaches its position before it could grow up. By decreasing the transfer matter coefficients β_u [Figs. 1(C1)–1(C3)], not enough chemicals reach the liquid layer to initiate a wave front and only a small bump at the interface is originated. This gives rise to two counter-rotating vortices that remain nicely traveling with the front at the same speed without perturbing its propagation.

The values of the transfer matter coefficients and σ turn out to be fundamental to control fluid vortex formation in the liquid and the onset of wave propagation in the liquid medium. Figure 2 shows the critical values of the transfer matter coefficients β_u and β_v for wave propagation in the liquid

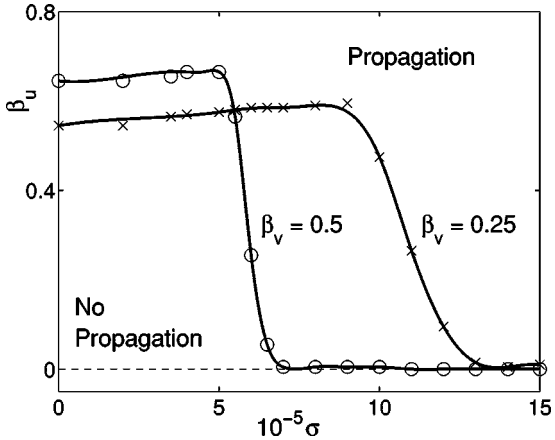

FIG. 3. Critical values of β_u versus σ. Two cases are plotted, namely, $\beta_v = 0.25$ (marked with $\times$) and $\beta_v = 0.5$ (marked with $\bigcirc$). (Solid lines are just a guide for the eye).

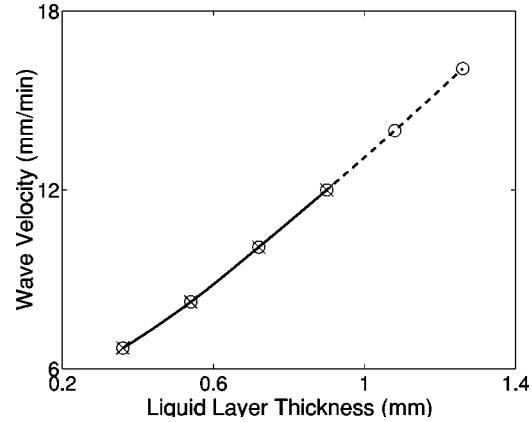

FIG. 4. Wave velocity in the liquid medium versus the thickness of the liquid layer. Two cases are plotted in the figure; $\beta_u = \beta_v = \beta_w = 0.0$ (marked with ($\times$) and a solid line; here gel and liquid media are uncoupled) and $\beta_u = \beta_w = 0.6$, $\beta_v = 0.25$ (marked with $\bigcirc$ and a dashed line). ($\sigma = 2.0 \times 10^{-5}$, wave velocity in the gel medium = 4.4 mm/min). (Solid and dashed lines are linear fits of the data with slope equal to 10.5 min^{-1}). Velocities were calculated by linearly fitting, once the stationary regime is achieved, all the x coordinates of the wave front versus time.

medium. Below the lines, the wave front in the gel is unable to excite a front in the liquid. It is interesting to note that independently of the specific values of σ, increasing the transfer matter coefficients of [ferroin], β_v, through the interface necessarily means that higher values of β_u are needed in order to achieve front propagation into the liquid medium.

On the other hand, in Fig. 3 the effect of σ for wave propagation is analyzed for two values of β_v. The lines correspond to the critical values of β_u above which wave propagation in the liquid medium occurs. For any value of β_v the behavior is equivalent to those two examples shown here, namely, a nearly constant value of β_u, and then a rapid drop in β_u to zero for some critical value σ_c. For any value of β_v contant, such the $\sigma > \sigma_c$ still holds, any value of β_u will give rise to front propagation in the liquid and finally this wave will be broken due to convection giving rise to multiple excitations in the gel surface as it was described above in Figs. 1(B1)–1(B3). Within the region of front propagation, for a constant value of β_u, as the coupling between hydrodynamics and the reaction dynamics of the Oregonator model is increased (i.e., σ increases), the wave front velocity increases due to the presence of two counter rotating vortices traveling with the wave. Note as well that the values of σ found in the literature [4], are usually quite below these critical values of σ_c but still open new possibilities for the effect of convection cells on pattern formation.

Finally, the role of the liquid layer depth for wave propagation has been investigated. Figure 4 shows the wave velocity in the liquid medium as a function of the layer depth for two different cases: (i) either the chemical transfer at the interface is allowed ($\beta_u \neq 0$ and $\beta_v \neq 0$) or (ii) is not allowed to occur ($\beta_u = \beta_v = 0$). In all cases, these velocities were higher than the wave front velocity in the gel layer due to the used diffusion coefficients. When $\beta_u \neq 0$ and $\beta_v \neq 0$, the wave front in the liquid keeps its shape (so wave velocity can be defined) for layers as deep as 1.26 mm. For higher depths, convective cells destroy the front and induce some kind of turbulence behavior as it was described above. When the chemical transfer at the interface is not allowed to occur, the maximum depth for steady wave propagation is 0.9 mm. Nevertheless, in both cases, the obtained wave velocities in the liquid medium were the same. The coupling of both media, gel, and liquid, induces a higher stability of the front dynamics which is translated into the need of higher depths in order to get higher convective cells able to destroy the wave front.

IV. DISCUSSION

Convective structures associated with traveling wave fronts in a two-layer medium have been observed and their properties analyzed in terms of mass transfer rate between both media, liquid layer width, and coupling strength σ between fluid flow and chemical dynamics. As a consequence of different chemical compositions in the vicinity of the front in the liquid medium, density gradients are induced giving rise to the formation of two counter rotating convective rolls. These cells move together with the wave front for small values of the mass transfer rate at the interface, while a disordered, otherwise turbulent, behavior is observed for higher values of β_u and β_v. The effects of transfer matter coefficients and σ on wave propagation are binded together. For a constant value of σ, increasing the transfer matter coefficient of [ferroin], β_v, necessarily means to increase β_u to achieve wave propagation. Nevertheless, for high enough values of σ, above some critical value σ_c, any value of β_u will give rise to wave propagation.

Previous experiments and numerical simulations taking into account convection have been performed only in aqueous solutions. Most of the actual experiments are performed in a two-layer media where wave propagation only takes place in the gel (catalyzer is immobilized in the gel). Here, we have shown that independently of the transfer rate at the interface, when the fluid flow dynamic is coupled to the chemical reaction kinetics, two counter-rotating vortices develop in the vicinity of the front. Even in the case of no front propagation in the liquid, a small perturbation at the gel surface gives rise to two convective cells. These results could be

verified by doing experiments with a BZ reaction whose catalyzer is then immobilized into the gel.

Although simulations in this paper are constrained to the 2D case, problems in 3D (a 2D gel covered by liquid) may also be studied. In this case, interesting phenomena coupling convection and diffusion may be observed [23].

ACKNOWLEDGMENTS

We acknowledge helpful comments by Dr. M. Gómez-Gesteira. This work was supported by DGES and Xunta de Galicia under Research Grant Nos. PB97–0540 and XUGA–20602B97, respectively.

[1] M.C. Cross and P.C. Hohenberg, Rev. Mod. Phys. **65**, 851 (1993).

[2] *Chemical Waves and Patterns*, edited by R. Kapral and K. Showalter (Kluwer Academic, Dordrecht, 1993).

[3] S. Chandrasekar, *Hydrodynamic and Hydromagnetic Stability* (Oxford University Press, Oxford, 1961).

[4] J.A. Pojman and I.R. Epstein, J. Phys. Chem. **94**, 4966 (1990); J.A. Pojman, I.R. Epstein, T.J. McManus, and K. Showalter, *ibid.* **95**, 1299 (1991); J. Masere, D.A. Vasquez, B.F. Edwards, J.W. Wilder, and K. Showalter, *ibid.* **98**, 6505 (1994).

[5] G. Bazsa and I.R. Epstein, J. Phys. Chem. **89**, 3050 (1985); J.A. Pojman and I.R. Epstein, *ibid.* **95**, 1306 (1991); I. Nagypal, G. Bazsa, and I.R. Epstein, J. Am. Chem. Soc. **108**, 3655 (1986).

[6] D.A. Vasquez, B.F. Edwards, and J.W. Wilder, Phys. Rev. A **43**, 6694 (1991); D.A. Vasquez, J.W. Wilder, and B.F. Edwards, Phys. Fluids A **4**, 2410 (1992); D.A. Vasquez, J.W. Wilder, and B.F. Edwards, J. Chem. Phys. **98**, 2138 (1993); J.W. Wilder, D.A. Vasquez, and B.F. Edwards, Phys. Rev. E **47**, 3761 (1993); D.A. Vasquez, J.M. Littley, J.W. Wilder, and B.F. Edwards, *ibid.* **50**, 280 (1994); Y. Wu, D.A. Vasquez, B.F. Edwards, and J.W. Wilder, *ibid.* **51**, 1119 (1995).

[7] V.N. Biktashev, A.V. Holden, M.A. Tsyganov, J. Brindley, and N.A. Hill, Phys. Rev. Lett. **81**, 2815 (1998).

[8] A.P. Muñuzuri, V. Pérez-Muñuzuri, M. Gómez-Gesteira, V.I. Krinsky, and V. Pérez-Villar, Int. J. Bifurcation Chaos Appl. Sci. Eng. **4**, 1245 (1994); A.P. Muñuzuri, V.A. Davydov, V. Pérez-Muñuzuri, M. Gómez-Gesteira, and V. Pérez-Villar, Chaos, Solitons and Fractals **7**, 585 (1996); M. Gómez-Gesteira, J. Mosquera, V.A. Davydov, V. Pérez-Muñuzuri, A.P. Muñuzuri, V.G. Morozov, and V. Pérez-Villar, Phys. Lett. A **231**, 389 (1997); H. Sevcikova, J. Kosek, and M. Marek, J. Phys. Chem. **100**, 1666 (1996).

[9] H. Miike, S.C. Müller, and B. Hess, Chem. Phys. Lett. **144**, 515 (1988); Phys. Rev. Lett. **61**, 2109 (1988); Phys. Lett. A **141**, 25 (1989); H. Miike, H. Yamamoto, S. Kai, and S.C. Müller, Phys. Rev. E **48**, 1627 (1993).

[10] B. McCaughey, J.A. Pojman, C. Simmons, and V.A. Volpert, Chaos **8**, 520 (1998).

[11] K.I. Agladze, V.I. Krinsky, and A.M. Pertsov, Nature (London) **308**, 834 (1984).

[12] M. Markus, G. Kloss, and I. Kusch, Nature (London) **371**, 402 (1994); M. Markus and K. Stavridis, Int. J. Bifurcation Chaos Appl. Sci. Eng. **4**, 1233 (1994).

[13] Q. Ouyang and J.M. Fleselles, Nature (London) **379**, 143 (1996).

[14] W. Jahnke, W.E. Skaggs, and A.T. Winfree, J. Phys. Chem. **93**, 3761 (1989); W. Jahnke and A.T. Winfree, Int. J. Bifurcation Chaos Appl. Sci. Eng. **1**, 445 (1991).

[15] J. Tyson and P.C. Fife, J. Chem. Phys. **73**, 2224 (1980); J.J. Taboada, A.P. Muñuzuri, V. Pérez-Muñuzuri, M. Gómez-Gesteira, and V. Pérez-Villar, Chaos **4**, 519 (1994).

[16] J. Tyson and J.P. Keener, Physica D **32**, 327 (1988).

[17] J.P. Keener and J. Tyson, Physica D **21**, 307 (1986).

[18] T. Plesser, H. Wilke, and K.H. Winters, Chem. Phys. Lett. **200**, 158 (1992).

[19] Z. Nagy-Ungvarai, S.C. Müller, T. Plesser, and B. Hess, Naturwissenschaften **75**, 87 (1988).

[20] C. Vidal and A. Noyau, J. Am. Chem. Soc. **102**, 6666 (1980); J. Boissonade, J.C. Roux, H. Saadaoui, and P. de Kepper, *Non-Equilibrium Dynamics in Chemical Systems*, edited by C. Vidal and A. Pacault (Springer-Verlag, Berlin, 1984).

[21] W.H. Press, S.A. Teukolsky, W.T. Vetterling, and B.P. Flannery, *Numerical Recipes in C*, 2nd ed. (Cambridge University Press, Cambridge, 1992).

[22] A.M. Zhabotinsky, M.D. Eager, and I.R. Epstein, Phys. Rev. Lett. **71**, 1526 (1993).

[23] V. Pérez-Villar *et al.* (unpublished).